Comparisons between perturbative and radiation-damped *R*-matrix approaches to dielectronic recombination: Application to Ar^{15+}

T. W. Gorczyca
Department of Physics, Western Michigan University, Kalamazoo, Michigan 49008-5151

F. Robicheaux and M. S. Pindzola
Department of Physics, Auburn University, Auburn, Alabama 36849-5311

N. R. Badnell
Department of Physics and Applied Physics, University of Strathclyde, Glasgow G4 0NG, United Kingdom
(Received 7 March 1996)

We apply a recently formulated close-coupling technique [Robicheaux *et al.*, Phys. Rev. A **52**, 1319 (1995)], which includes radiation damping via an optical potential, to the calculation of dielectronic recombination cross sections of Ar^{15+}. Specifically, we compare the results from both Wigner-Eisenbud and eigenchannel *R*-matrix calculations to perturbative methods. For this system, no evidence for interfering resonance phenomena is found, and excellent agreement is obtained among all methods. This indicates that the present close-coupling treatment of the dielectronic recombination is highly accurate and can therefore be used to investigate systems where lower-order perturbative methods are inappropriate, such as where interference effects between neighboring resonances and between direct and resonant recombination processes are expected. [S1050-2947(96)02709-6]

PACS number(s): 34.80.Kw

I. INTRODUCTION

Dielectronic recombination (DR), the process by which an atomic ion captures a free electron into a doubly excited state, and subsequently decays by spontaneously emitting a photon, is an important cooling mechanism in hot plasmas [1,2]. As such, it has received a considerable amount of attention, both theoretically and experimentally [3]. On the experimental side, among other methods, crossed-beam measurements at the accelerator-cooler ring facility at Aarhus [4] have determined DR cross sections for many low- to moderately charged ions at fair energy resolution [3]. Due to the recent lowering of the electron-beam transverse temperature [5], considerably higher-resolution measurements of DR are now possible [6]. In addition, with the advent of the electron-beam ion trap (EBIT), fully stripped U^{92+} ions have been produced [7]. By detecting x rays, rather than just counting the recombined ions as is done for crossed- and merged-beams methods [3], partial DR cross sections to selected energy ranges of final decay states can be observed, as was done recently for highly charged uranium ions [8].

In actual experiments, the measured quantity is the total photorecombination (PR) cross section, which is the coherent admixture of DR and the nonresonant process radiative recombination (RR). Since the dominant observable features are usually just the resonant part, however, we shall speak in terms of DR cross sections alone, assuming that the RR contribution is included as well. Theoretical calculations for DR are usually based on one of two methods. The first class consists of perturbative methods [9], that have been quite successful in reproducing observed DR cross sections. The common implementation of this method, the isolated-resonance, independent-processes approximation [10–13], neglects higher-order effects such as resonance-resonance and resonance-background interferences, the background being RR. Although these effects may be included in principle [14–17], a general scheme for incorporating interference effects between entire Rydberg series does not exist. Even so, a recent third-order perturbative study for low-lying resonances [17] showed that resonance-background interference effects, while not important for total DR cross sections, were significant for *partial* DR cross sections, which is precisely what is measurable when detecting x rays from the EBIT facility [8]. As for resonance-resonance interference, it has been demonstrated for electron-ion excitation that when members of different Rydberg series coincide closely in energy, the resonance profile can be dramatically altered [18]. Further, as will be pointed out in Sec. II A, the energy-averaged DR cross sections at lower charges and low electron-energy resolution depend only on the radiative widths Γ_r, independent of the autoionization widths Γ_a. The relative positions of these resonances are likewise smeared out when energy averaged with a broad distribution function. Thus, possible inaccuracies in the calculated resonance positions and widths will not be seen when comparing theory and experiment. For higher-resolution experiments, however, the measured and (convoluted) theoretical resonance structure will reveal more detailed, Γ_a-dependent features.

In view of the existing higher-charged, higher-resolution experimental capabilities, it is desirable to rely on a theoretical method which includes interference effects to all orders and most accurately computes autoionization widths Γ_a, and resonance positions E_R. The second class of theoretical methods for handling DR makes use of the close-coupling method [19], which automatically includes all orders of these interference processes, and provides a more reliable estimate of the autoionization widths as well. Davies and Seaton, us-

ing an *ab initio* treatment based on a time-dependent expansion of the total wave function [20], derived an exact expression for the electron-electron (elastic or inelastic scattering) and electron-photon (radiative or dielectronic recombination) scattering matrices $\mathbf{S}_{ee}$ and $\mathbf{S}_{ep}$, respectively, the evaluation of which, however, requires knowledge of the dipole matrices along all points on a certain contour in the complex plane. For higher-n resonances, a quantum-defect theory (QDT) method, as formulated by Bell and Seaton [21], simplified the expression considerably and was first applied to the damping of resonances in the electron-impact excitation of O^{6+} by Pradhan and Seaton [22]. At lower n, where this approximation is not valid, the original formulation of Davies and Seaton [20] has been implemented only once to our knowledge. For the case of photoionization of Fe^{24+} (analogous to DR of Fe^{25+}; see below), the dipole matrices were parametrized and analytically continued into the complex plane, enabling the evaluation of the necessary contour integrals [23].

Another method used for treating DR to low-lying states [24] calculates photoionization cross sections from each low-lying state to the pertinent electron continua, and uses the detailed balance relation

$$\sigma_{DR}=\sigma_{PI}\frac{g_i}{g_f}\frac{\omega^2}{c^2k^2} \tag{1}$$

to obtain the partial DR cross section σ_{DR} to each final state, where σ_{PI} is the partial photoionization cross section, the $g_{i(f)}$ are the statistical weights of the initial (final) states, ω is the photon frequency, and k is the electron momentum. The implementation of this method [24] is to calculate photoionization cross sections using final-state continua determined in the absence of the radiative field. Thus the widths of the resonances include only the autoionization widths and neglect the radiative widths. For low-Z ions, for which the autoionization widths Γ_a are typically orders of magnitude larger than the radiative widths Γ_r, there is no difficulty with this prescription. However, as is well known, the Γ_r increase much faster than the Γ_a as the residual charge Z on the ion increases [9]. At some point, the neglect of the radiative width leads to a severe underestimate of the total width, and therefore a corresponding overestimate of the DR cross section. This follows from considering the perturbative expression (see Sec. II A): the radiation-damped DR cross section is given by

$$\sigma_{DR}\sim\frac{\Gamma_a\Gamma_r}{(E-E_R)^2+\left(\frac{\Gamma_a+\Gamma_r}{2}\right)^2}, \tag{2}$$

whereas neglect of the radiative width in the continuum-plus-resonance wave function is equivalent to replacing the $\Gamma_a+\Gamma_r$ term in the denominator of Eq. (2) with just Γ_a.

The limitations of these close-coupling methods for treating DR meant that, at least for highly charged ions, the only theoretical methods available were those based on perturbation theory. Recently, however, a R-matrix method incorporating radiation damping was formulated by Robicheaux *et al.* [25] and has been applied to the electron-impact excitation resonances in heliumlike Ti^{20+} [26], and hydrogenic Fe^{25+} and Mo^{41+} [27]. It was proven that this method is equivalent to the general formulation of Davies and Seaton [20]. Thus it reduces to the QDT method of Bell and Seaton [21] in the appropriate limit of intermediate n (in the limit $n\to\infty$, the Bell and Seaton expression for damping deviates from the more rigorous expression of Robicheaux *et al.* [25], although the n for which this occurs is so large as to be of little practical interest). More importantly, it is valid for low-lying resonances, for which the decay occurs at small electron radii. For this case, the matrix elements of the R-matrix Hamiltonian acquire an additional, imaginary potential. This gives rise to the damping, but also modifies the total width by inclusion of the radiative widths. As previously pointed out, for high Z this radiative contribution is crucial for determining the correct resonance structure.

The application of the theoretical method of Robicheaux *et al.* [25] towards the calculation of DR cross sections is the central theme of this paper, and will be presented as follows. In Sec. II, we describe the various theoretical treatments of the DR process. In particular, the standard equations of perturbation theory, which are used in the present calculations for comparison purposes and also to garner insight into the present close-coupling results, are outlined in Sec. II A. In Sec. II B, the modifications to two different R-matrix codes are summarized as they apply to the present test case DR of Ar^{15+} and the different types of damping are discussed. We then compare R-matrix and perturbative calculations for this test case in Sec. III, followed by concluding remarks in Sec. IV. Atomic units (a.u.) are used throughout unless otherwise specified.

II. THEORETICAL METHODS

A. Perturbative considerations

For the perturbative calculations presented in this paper, we used the two codes AUTOSTRUCTURE [28] and DRFEUD [29], which apply standard perturbation theory [9] in the isolated-resonance, independent-processes, distorted-wave approximation [13]. For simplicity in understanding the behavior of the DR cross section, we consider the case of one resonance embedded in one continuum, with allowed decay to one recombined (bound) state. The energy dependence of the cross section can then be written as

$$\sigma_{DR}(E)=\frac{\pi}{k^2}\frac{(2J+1)}{2(2J_t+1)}\left[\frac{\Gamma_a\Gamma_r}{(E-E_R)^2+\left(\frac{\Gamma_a+\Gamma_r}{2}\right)^2}\right], \tag{3}$$

where $E=k^2/2$ is the electron energy, J and J_t are the total angular momenta of the electron-plus-target and target, respectively, E_R is the resonance position,

$$\Gamma_a=2\pi\left|\left\langle\Psi_c\left|\sum_{i,j>i}\frac{1}{r_{ij}}\right|\Psi_R\right\rangle\right|^2 \tag{4}$$

is the autoionization width, computed using an energy-normalized distorted wave coupled to a target wave function to represent the continuum wave function Ψ_c, and a bound-state wave function for the resonance Ψ_R, and

$$\Gamma_r=\frac{4\omega^3}{3c^3}\left|\left\langle \Psi_b\left|\sum_i \vec{r}_i\right|\Psi_R\right\rangle\right|^2 \tag{5}$$

is the radiative width for spontaneous decay, with photon energy ω, of the resonance to a bound state described by the wave function Ψ_b. The above expression, when energy averaged over a bin of width $\Delta\epsilon$, becomes

$$\langle\sigma\rangle=\frac{2\pi^2}{\Delta\epsilon k^2}\frac{(2J+1)}{2(2J_t+1)}\frac{\Gamma_a\Gamma_r}{\Gamma_a+\Gamma_r}. \tag{6}$$

At lower stages of ionization, where $\Gamma_a\gg\Gamma_r$, the above expression depends only on Γ_r and is independent of Γ_a.

The bulk of the work in the recent past relied on these perturbative methods to compare with experiment. The obvious next step in obtaining more accurate theoretical results is to go beyond the isolated-resonance, independent-processes, distorted-wave approximation by incorporating channel coupling and various interference effects into the calculations, which are routinely included in close-coupling calculations.

B. *R*-matrix methods

The particular type of close-coupling [19] calculations we use are based on the *R*-matrix method [30,31]. One of two sets of codes is used in this paper. The first is the Belfast suite of *R*-matrix codes which were first written for the Opacity Project [32], and have more recently been modified [33] by including relativistic corrections to the Hamiltonian, [34,35] in order to study ions of interest to the Iron Project [36]. A Wigner-Eisenbud boundary condition is applied at the *R*-matrix surface [30,31]. The second set is the Colorado suite of codes [37], which use instead an eigenchannel approach. The two program packages have undergone a detailed comparison to one another for the case of photoionization of barium [38], where it was found that both codes reproduced experimental measurements provided that a sufficiently converged basis of configurations, consisting of appropriate orbitals, was used.

The modification of any close-coupling method, and, in particular, the *R*-matrix method, to handle various types of radiation damping has been previously described in detail [25]. Additional modifications pertaining only to the Belfast suite of codes have also been described [26]. Nonetheless, for the purpose of elucidating these processes as they apply to our present test case, we briefly review the essential points.

When an electron incident on the $2s_{1/2}$ ground state of Ar^{15+} is captured into a resonance state, a process known as dielectronic capture,

$$e^-+1s^22s_{1/2}\rightarrow 1s^22p_jnl \text{ dielectronic capture } (j=1/2,3/2),\quad (n\geqslant 10), \tag{7}$$

there are several decay pathways available to this resonance, given by

$$1s^22p_jnl\rightarrow 1s^22s_{1/2}+e^- \text{ elastic scattering}, \tag{8a}$$

$$\rightarrow 1s^22p_{1/2}+e^- \text{ excitation } (j=3/2), \tag{8b}$$

$$\rightarrow 1s^22l2l'+\hbar\omega \text{ inner-region damping}, \tag{8c}$$

$$\rightarrow 1s^22s_{1/2}nl+\hbar\omega \text{ type I damping}, \tag{8d}$$

$$\rightarrow 1s^22p_jn'(l\pm 1)+\hbar\omega \text{ type II damping } (3\leqslant n'\leqslant 9). \tag{8e}$$

The first two processes Eqs. (8a),(8b) give rise to the autoionization widths of the resonance into the initial or excited continua,

$$\Gamma_a^i=2\pi\left|\left\langle 1s^22p_jnl\left|3\left(\frac{1}{r_{13}}+\frac{1}{r_{23}}\right)\right|1s^22s_{1/2}k_il_i\right\rangle\right|^2, \tag{9}$$

where i now denotes the particular electron continuum with linear and angular momenta k_i and l_i, the orbitals for which are energy normalized: $\langle k_il_i|k_{i'}l_{i'}\rangle=\delta(k_i^2/2-k_{i'}^2/2)\,\delta_{ii'}\,\delta_{l_il_{i'}}$. The last three Eqs. (8c)–(8e) together with the dielectronic capture Eq. (7) constitute the DR process. Equation (8c) is termed inner-region damping to differentiate it from the other types because the final decay states are all (necessarily) contained within the *R*-matrix ''box.'' These final states are usually highly correlated, so that a simple one-electron description for this type of decay is insufficient. We include this type of decay by adding a radiative optical potential to the Hamiltonian [25]

$$V_{rad}=-i\sum_b\frac{2\omega_b^3}{3c^3}D|b\rangle\langle b|D, \tag{10}$$

where $\omega_b=E-E_b$ is the energy difference between energies of the scattering and final states, $D=\Sigma_{s=-1}^{s=1}r_sC_s^1$ is the dipole operator, C_m^λ is the renormalized spherical harmonic $C_m^\lambda=\sqrt{4\pi/(2\lambda+1)}Y_m^\lambda$ and $|b\rangle$ represents a normalized final state. This potential contributes an additional term to the Hamiltonian matrix

$$H_{\alpha\alpha'}\rightarrow H_{\alpha\alpha'}-i\sum_b\frac{2\omega_b^3}{3c^3(2J+1)}\langle\alpha||r||b\rangle\langle b||r||\alpha'\rangle, \tag{11}$$

leading to a nonunitary **S** matrix. The photorecombination cross section within a partial wave is then proportional to this degree of nonunitarity

$$\sigma_{PR}=\frac{\pi}{k^2}\frac{(2J+1)}{2(2J_t+1)}\sum_{i=1}^{n_1}\left(1-\sum_{j=1}^{n_t}S_{ij}^*S_{ij}\right), \tag{12}$$

where J is the total partial-wave angular momentum, $J_t=1/2$ is the angular momentum of the $2s_{1/2}$ target state, n_t is the total number of open channels, and n_1 is the number of channels coupled to the $2s_{1/2}$ target state. Also, this modification to the *R* matrix yields the portion of radiative recombination

$$e^-+1s^22s_{1/2}\rightarrow 1s^22s_{1/2}2l_j. \tag{13}$$

The type I damping shown in Eq. (8d) has neither the initial resonance nor the final state completely contained in the *R*-matrix ''box,'' and so simply modifying the *R*-matrix Hamiltonian will not suffice. As originally suggested by

Hickman [39], and derived within the present radiative optical potential approach by Robicheaux *et al.* [25], this type of damping can be incorporated by modifying the binding energy of the valence orbital according to

$$\epsilon_{nl} \rightarrow \epsilon_{nl} - i\frac{\Gamma_{2p_j \rightarrow 2s_{1/2}}}{2}, \tag{14}$$

where nl are the quantum numbers of the valence orbital with binding energy ϵ_{nl}, $j=1/2$ or $3/2$ depending on the core state to which the valence electron is attached, and $\Gamma_{2p_j \rightarrow 2s_{1/2}}$ are the core radiative widths from the appropriate capture state to the ground state. This modification leads to a complex effective quantum number $\nu_c = \nu/\sqrt{1 - i\Gamma\nu^2/Z^2}$, which, when used within a QDT approach to scattering, gives rise to a nonunitary **S** matrix

$$\mathbf{S} = \mathcal{S}_{oo} - \mathcal{S}_{oc}(\mathcal{S}_{cc} - e^{-2\pi i \nu_c})^{-1}\mathcal{S}_{co}. \tag{15}$$

An alternative method for treating this type of damping [26], which is necessary when using the Belfast R-matrix codes in their usual treatment of asymptotics for closed channels [32,40,41], is to modify the asymptotic energy of the closed-channel, exponentially decaying solutions $\theta(r)$ and $\dot{\theta}(r)$ [41]. Use of these solutions alone automatically gives rise to the physical scattering matrix **S** in Eq. (15) [41]. They are given by the asymptotic expansion

$$\theta(r) = r^{\nu} e^{-Zr/\nu} \sum_n B_n r^{-n}, \tag{16}$$

and

$$\dot{\theta}(r) = \frac{d\theta(r)}{dE} = \left(\frac{\nu^3}{2Z^2}\right)\frac{d\theta(r)}{d\nu}, \tag{17}$$

where the coefficients B_n are computed by standard asymptotic recurrence relations [41]. The modification $\nu_c = \nu/\sqrt{1 - i\Gamma\nu^2/Z^2}$ just requires that the evaluation of $\theta(r)$ and $\dot{\theta}(r)$ is done instead for complex ν_c [26]. Two important differences between this asymptotic modification and the QDT method are as follows.

Firstly, in the Belfast codes, use of the closed-channel solutions vs the QDT $s(r)$ and $c(r)$ solutions (see Refs. [42,41,26]) is found to be one to two orders of magnitude faster per evaluation. When the QDT solutions need to be evaluated at every energy, for instance, at low-n resonances where the various unphysical matrices in Eq. (15) have strong energy dependence, the QDT method is much slower for total scattering runs. However, at higher n where there is little energy dependence in these matrices, only a few actual evaluations are required using the QDT method, and Eq. (15) alone can be interpolated for intermediate energy points. When detailed, narrow resonance structure must be mapped out, perhaps millions of energy points are needed, making the QDT method, in such cases, orders of magnitude faster than the asymptotic modification method.

Secondly, using $\theta(r)$ and $\dot{\theta}(r)$ within the Belfast method leads to a straightforward inclusion of long-range dipole and quadrupole potentials via first-order perturbation [32,41], but using these same techniques to perturb negative-energy $s(r)$ and $c(r)$ solutions is invalid since both these solutions diverge as $r \rightarrow \infty$. Furthermore, in the present case, at energies just above the $2s_{1/2}$ threshold the higher-l continuum orbitals have their radial point of inflection far outside the R-matrix ''box.'' As such, the Belfast treatment of perturbation between open and closed channels is inapplicable. In the Appendix, however, we outline a method for incorporating the long-range *dipole* perturbation between open and closed $s(r)$ and $c(r)$ solutions, and this method does not have either of the above numerical difficulties.

In the present case, for which it is necessary to resolve a large number of high-n (narrow width) resonances, we have elected to use the QDT method for treating type I damping in the Belfast codes (this is the normal mode of operation in the Colorado codes). As a consistency check, the Belfast codes with the asymptotic modification method was used in spot checks to verify that both methods yielded identical results; use of the asymptotic method at every energy would have led to an increase in computational time of a factor of ~ 1000 for the dense energy mesh used, however.

The type II damping shown in Eq. (8e) is a valence transition ($n \geqslant 10 \rightarrow n' = 3-9$) for which the outer electron does not overlap appreciably with the target ($n \leqslant 2$) orbitals. Thus the damping occurs mainly in the asymptotic region, and is treated perturbatively by either modifying the **K** matrix [25], or the outer-region solutions directly [26] when asymptotically decaying states $[\theta(r), \dot{\theta}(r)]$ [41] are used instead of QDT solutions. In the former case, the unphysical $\mathcal{K}$ matrix, which yields the unphysical $\mathcal{S}$ matrix in Eq. (15), is modified due to the diagonal perturbing potential

$$\mathcal{K}_{cc} \rightarrow \mathcal{K}_{cc} + i\sum_{n'=3}^{9} \sum_{l'=l\pm 1} \Gamma_{nl \rightarrow n'l'}/2, \tag{18}$$

where $\Gamma_{nl \rightarrow n'l'} = 4\pi\omega^3/3c^3(2J+1)|\langle nl||\vec{r}||n'l'\rangle|^2$ is the radiative width of the valence electron nl to each decay state $n'(l'=l\pm 1)$ calculated using either distorted waves in the Colorado codes [25], or hydrogenic orbitals in the implementation in the Belfast codes [26]. A similar perturbation to the $\mathcal{K}_{oo}$ diagonal elements incorporates the $e^- + 1s^2 2s_{1/2} \rightarrow 1s^2 2s_{1/2} n'l'$ RR contribution.

The implementation of either method for calculating DR cross sections is to perform scattering calculations for a range of energies, thereby producing nonunitary **S** matrices, and to use these in Eq. (12). A difficulty arises in fully resolving the many narrow resonances of entire Rydberg series, however. In the present case, the many LS-forbidden resonances have autoionization widths Γ_a, and therefore total widths, that are much narrower than the allowed ones. Inspection of Eq. (6), however, indicates that these narrow resonances can contribute just as much to the averaged DR cross section; see Ref. [27]. Thus if a linear mesh is used, the cross section must be computed at a very large number of energies in order to resolve all of the resonances. This differs considerably from the case of resonant electron-impact excitation where the narrowest resonances frequently make a proportionally small contribution to the cross section compared to the broadest resonances (see Ref. [27]) and/or they are completely damped (see, e.g., Ref. [26]) and thus, either way, it is unnecessary to resolve them.

A more sophisticated method for resolving all resonances up to some highest principal quantum number n_{max} is as follows. The Rydberg resonances are characterized by a quantum number n and quantum defect μ leading to an energy position $E_R \sim E_i - Z^2/2(n-\mu)^2$, and a total width (equal to the autoionization width, assuming $\Gamma_a \gg \Gamma_r$) which scales like $\Gamma_a \sim \Gamma_0/(n-\mu)^3$. There is, thus, a pole of the S matrix at the complex energy $E = E_i - Z^2/2(n-\mu)^2 - i\Gamma_a/2$, or equivalently, a zero in the determinant of the matrix $\mathcal{S}_{cc} - e^{-2\pi i \nu_c}$ in Eq. (15). While the exact quantum defects and widths deviate from these analytical forms at lower n due to the interaction between the $2p_{1/2}nl$ and $2p_{3/2}n'l'$ series, or equivalently, nondiagonal terms in the $\mathcal{S}$ matrix, one can search in the complex plane for the pole of the S matrix around the QDT-like values. Given the determined exact position E_R and width Γ_a, an energy mesh of 55 points is used, the positions given by

$$E_j = E_R + s_j \Gamma_a , \tag{19}$$

with

$$s_j = \begin{cases} j/5, & j = \pm 0 - 10 \\ s_{j-1}(1 + s_{j-1}/20), & j = \pm 11 - 25 \end{cases} \tag{20}$$

$$s_{\pm 26} = 4 s_{\pm 25} , \tag{21}$$

$$s_{\pm 27} = 8 s_{\pm 26} . \tag{22}$$

This mesh yields a sufficiently dense representation of the resonance profile (the latter two points are chosen so as to include the long $1/E^2$ tail of the Lorentzian), so that accurate energy-averaged resonance contributions to the DR cross section may be computed.

III. RESULTS

Dielectronic recombination of lithiumlike Ar^{15+} has been the subject of a recent joint experimental-theoretical study [43]. It was found that theoretical results for $\Delta n = 0$ DR using the code DRFEUD [29] gave excellent agreement with merged-beams results measured at the UNILAC of GSI at Darmstadt, at least for the lower-lying resonances. Measurements for the higher resonances were affected by external electric fields. We use these same theoretical results, as well as AUTOSTRUCTURE results based on the same working equations used by DRFEUD and outlined in Sec. II A, to compare to our two separate (Belfast and Colorado) R-matrix results. All these results are shown in Fig. 1. Some details of these calculations are summarized below.

While the R-matrix method implicitly includes RR, perturbative methods must add this independent contribution, which is done incoherently within the independent-processes approximation. Although the RR contribution can easily be calculated perturbatively, to simplify our comparisons for the resonances we determined this nonresonant background by performing Belfast R-matrix calculations including just the $2s_{1/2}kl$ ground-state continuum channel, thereby eliminating the resonance producing $2p_{1/2,3/2}nl$ channels. This yielded a smooth, resonance-free background cross section of the same magnitude as the full R-matrix calculation which was then added to the perturbative resonant contributions.

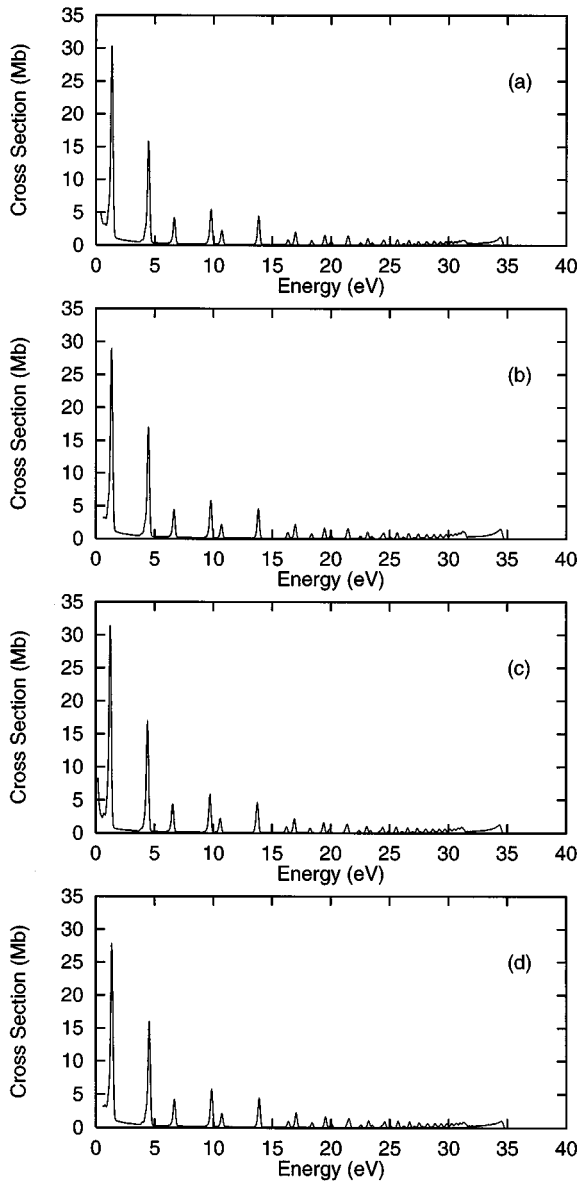

FIG. 1. Photorecombination cross sections for Ar^{15+}, including contributions up to $n = 75$, and convoluted with a 0.2 eV FWHM Gaussian: (a) Belfast R-matrix results; (b) AUTOSTRUCTURE results; (c) Colorado R-matrix results; (d) DRFEUD results.

For all calculations, we terminated each Rydberg series at $n = 75$. Due to inevitable external fields present in any experimental apparatus, there exists a highest principle quantum number n_{max} above which the Rydberg states are Stark shifted into the continuum, so that these higher states do not contribute to DR. In the previous study of Ar^{15+} [43], this value was chosen as $n_{max} = 64$, although the cross section was found to be insensitive to this precise value. For the present case we have taken this to be $n_{\max} = 75$ for all calculations. Finally, all cross sections in Fig. 1 were convoluted with an 0.2 eV full width at half maximum (FWHM) Gaussian profile. As $E \to 0$, however, this width is shrunk to zero in order to match smoothly onto the $1/E$ RR behavior below the $2p_{1/2}10l$ resonances.

From Fig. 1 it is seen that all four convoluted theoretical results compare favorably. This only indicates that the radia-

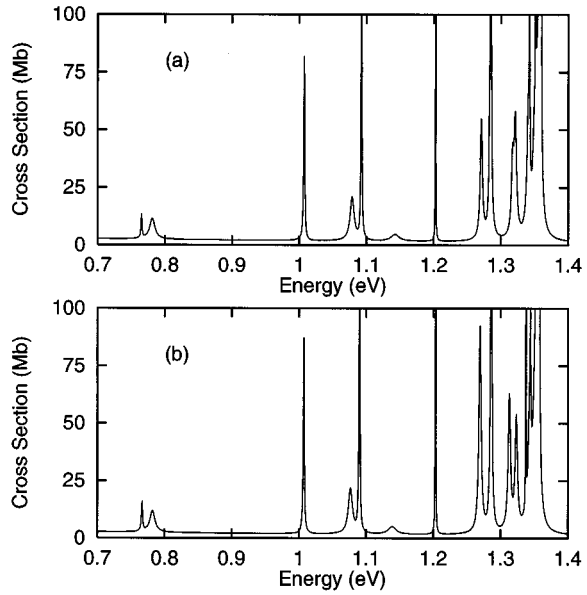

FIG. 2. Unconvoluted photorecombination cross sections in the $2p_{1/2}10l$ resonance region: (a) Belfast R matrix; (b) AUTOSTRUCTURE.

tive widths of the resonances are similar, however, since, by Eq. (6), the averaged cross section is independent of the autoionization width. Thus possible inaccuracies in the autoionization widths as well as the relative positioning between various resonances are not evident at this level of resolution. Further, the profiles seen in Fig. 1 represent the average radiative contribution from entire groups of resonances $2p_jnl$. In order to show that the resonance profiles are in fact the same between perturbative and R-matrix methods, we plot unconvoluted cross sections of the $2p_{1/2}10l$ resonance region in Fig. 2. Note that there is generally very good agreement at this level of resolution as well, indicating that the perturbative and R-matrix methods are modeling the DR process at the same level of accuracy.

It is interesting to investigate the dominant damping pathways for this DR process. In Fig. 3, we show DR cross sections including only one of the three contributions, inner-region damping, type I damping, or type II damping. Inner-region damping involves the quantity $\langle nl|r|2l'\rangle$, which tends to zero as $n\rightarrow\infty$. This is because the $\langle nl|2l'\rangle$ overlap itself is reduced considerably at $n>10$ and decreases with n. It also depends on the configuration interaction (CI) mixing within the $1s^22s_{1/2}2l$ and $1s^22p_j2l$ decay states. The type II damping has a similar decrease with n, but unlike inner-region damping it has many $3\leqslant n'\leqslant 9$ final decay states, and also has a greater overlap $\langle n'(l\pm1)|nl\rangle$ for any decay states. It thus accounts for a far greater contribution than the inner-region damping at all n. For type I damping, we first note that the radiative width Γ_r is n independent as $n\rightarrow\infty$, since only the core participates in the transition. Thus, at low and intermediate n where $\Gamma_a\gg\Gamma_r$, the energy-averaged cross section is constant for each resonance, or the binned cross section, using a bin width on the order of $1/n^3$, scales as n^3. The energy-averaged cross sections up to some $n=n_{max}$ thus behaves like $\sim n_{max}^3=Z/(E_{2p_j}-E)^{3/2}$ as $E\rightarrow E_{2p_j}$. At very high n, of course, the autoionization width

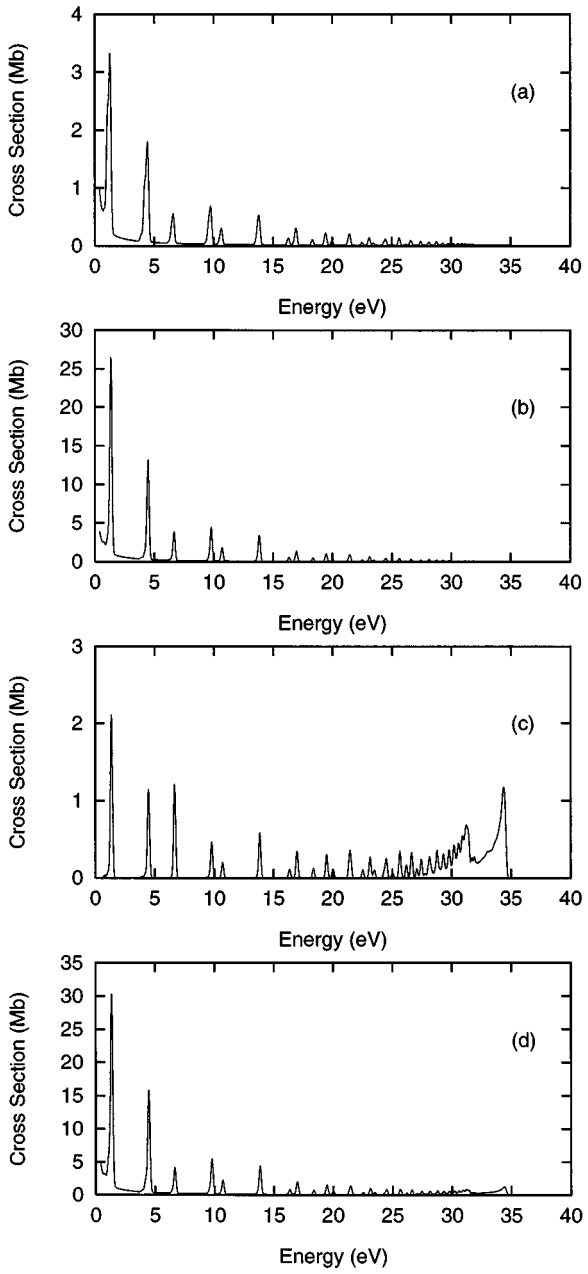

FIG. 3. Various contributions to the photorecombination cross section for Ar^{15+}: (a) inner-region damping; (b) type II damping; (c) type I damping; (d) total photorecombination cross section. All results are from Belfast R-matrix calculations, and are convoluted with a 0.2 eV FWHM Gaussian.

becomes less than the radiative width due to the $1/n^3$ scaling, and the energy-averaged DR cross section instead behaves as $1/n^3$, or the binned cross section approaches a constant. The behavior for each of these decays at the Rydberg limit is clearly seen in Fig. 3.

As mentioned in the previous section, the long-range contribution is expected to dominate at high l or low E. We show that this is indeed the case for the present system by focusing on the $J=6$ odd partial wave, with and without long-range perturbations. The results of both of these R-matrix calculations are shown in Fig. 4 in the region of the four $2p_{3/2}10l_{j=l\pm1/2}$ resonances ($l=4$, $j=9/2$, $l=6$, j

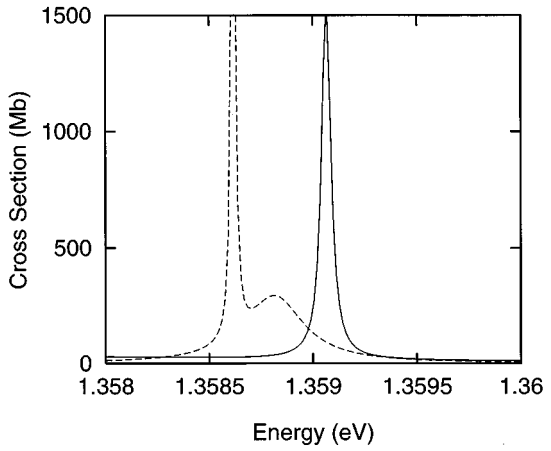

FIG. 4. The $2p_{1/2}10l$ $J=6$ odd partial-wave contribution to the photorecombination cross section for Ar15+. Solid line, present R-matrix results without long-range dipole perturbation; dashed line, results including long-range dipole perturbation. Both results are unconvoluted.

$=11/2$, $l=6$, $j=13/2$, and $l=8$, $j=15/2$). Since these resonances cannot be isolated further without eliminating channels, and therefore CI mixing, we are only able to study the sum of all four resonances, which, nevertheless, shows an obvious dependence on the long-range dipole potential. When the long-range dipole perturbation is included, the area under the DR cross-section curve, and therefore the energy-averaged DR cross section, increases. Over the entire DR range 0.4 eV$\leqslant E\leqslant$40 eV, shown in Fig. 5, we see that especially in the $2p_{3/2}10l$ resonance region, where the continuum energy is the smallest, the omission of long-range perturbations leads to a reduction from about 30 Mb to about 22 Mb

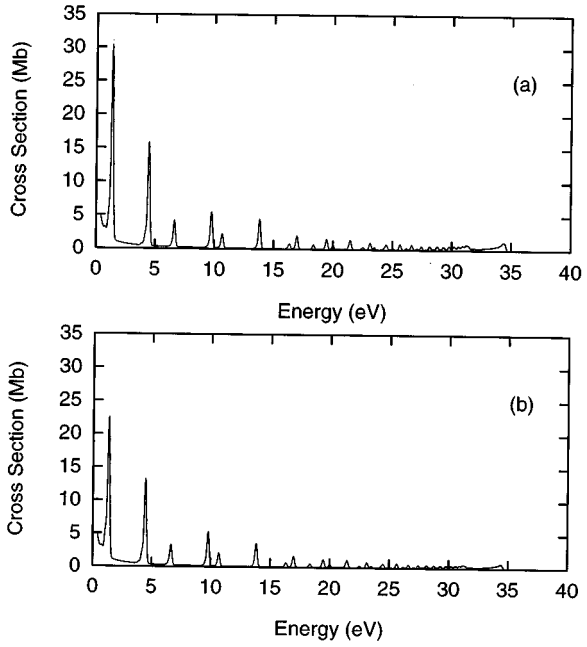

FIG. 5. Total photorecombination cross sections for Ar^{15+} (a) with and (b) without the long-range dipole perturbation included. Both results are from the Belfast R-matrix calculations, and are convoluted with a 0.2 eV FWHM Gaussian.

for the peak cross section. This reduction lessens for intermediate n (higher continuum energies), but increases again at the high-n limit, where instead the resonance states nl now have little probability of being found in the inner region.

IV. CONCLUSION

We have successfully implemented the close-coupling treatment of photorecombination for the relatively simple system of electrons incident on lithiumlike Ar^{15+}. Using the formulation of Robicheaux *et al.* [25], we modified two separate R-matrix codes, the Belfast and Colorado versions, and found excellent agreement between these two and between the two perturbative codes AUTOSTRUCTURE and DRFEUD for the $\Delta n=0$ DR cross sections. It was found that inclusion of long-range perturbative effects within the R-matrix method was necessary to compute correct autoionization widths, as was a sophisticated search method for resolving all of the many narrow resonances. The present method was also shown to be superior to methods based on inverse-photoionization calculations for decay to low-lying recombined states since the radiative width is incorporated into the total width via an optical potential.

The validity of the present R-matrix approach for treating DR paves the way for new investigations of systems where standard perturbation codes are expected to break down, namely, where various higher-order interference effects are required. These include DR of highly charged ions, especially to selected final decay states, where resonant and background contributions sum incoherently, and also for cases of near degeneracy of Rydberg resonances from different series. Existing discrepancies between past experimental and perturbative theoretical results may benefit from studies which include all-order interference effects. For very highly charged ions, these semirelativistic methods will need to be extended to include relativistic effects. Using the similar DARC R-matrix codes that incorporate these relativistic effects, [44,45] and the modifications detailed here, this should be a straightforward task. Inclusion of the Breit interaction in relativistic R-matrix codes remains the final ingredient toward the treatment of DR of the highest-charged ions capable of being studied experimentally, currently, U^{91+}.

ACKNOWLEDGMENTS

T.W.G. and M.S.P. were supported in part by the U.S. Department of Energy, Office of Fusion Energy, under Contract No. DE-FG05-86-ER53217 with Auburn University. F.R. was supported by NSF Grant No. NSF-PHY-9457903, and N.R.B. was supported in part by EPSRC Contract No. GR/K/14346 with the University of Strathclyde.

APPENDIX: LONG-RANGE PERTURBATIONS WITH UNPHYSICAL CLOSED-CHANNEL SOLUTIONS

A necessary ingredient for calculating accurate DR cross sections within the R-matrix method, as mentioned in Sec. II B, is the perturbative inclusion of the long-range dipole potential. This turns out to be important in the present case because, as can be seen in Eq. (9), the autoionization widths Γ_a depend on a (predominantly) dipole coupling matrix between the initial continuum state $2s_{1/2}kl'$ and the resonant

state $2p_j nl$. The portion of this integral inside the R-matrix box ($0 \leq r \leq r_A$) is automatically handled to all orders via the R matrix itself. Outside the box, since we are dealing with a multiply charged ion, a first order perturbative treatment is sufficient [32]. This latter contribution becomes especially important in one of two cases. When either (1) the initial continuum state resides mostly outside the box, as is the case for either low energies or high angular momenta, corresponding to a classically allowed region outside the box only, or (2) the resonance state resides mostly outside the box, as is the case for high n, then the inner-region contribution to the autoionization width is negligible. In order to compute perturbative corrections to the **K** matrix, or to the solutions themselves, the following four quantities are needed:

$$\int_{r_A}^{\infty} dr s_o(r) \frac{\alpha}{r^2} s_c(r), \tag{A1a}$$

$$\int_{r_A}^{\infty} dr s_o(r) \frac{\alpha}{r^2} c_c(r), \tag{A1b}$$

$$\int_{r_A}^{\infty} dr c_o(r) \frac{\alpha}{r^2} s_c(r), \tag{A1c}$$

$$\int_{r_A}^{\infty} dr c_o(r) \frac{\alpha}{r^2} c_c(r), \tag{A1d}$$

where the subscripts o and c indicate that the Coulomb functions $s(r)$ and $c(r)$ refer to open and closed channels, respectively. Each of the closed-channel solutions diverges exponentially as $r \to \infty$ on the real axis but the final physical solutions will be a linear combination of these which go to zero asymptotically (see below). We can thus compute the part of each of these four integrals that will remain after this linear combination is formed as follows. First, we form the solution

$$e_o^+(r) = c_o(r) + i s_o(r), \tag{A2}$$

which has the asymptotic property

$$e_o^+(r) \underset{r \to \infty}{\to} e^{+\xi(r)}, \tag{A3}$$

where $\xi(r) = ikr + z/k \ln 2kr + il\pi/2 + \sigma_l$ and $\sigma_l = \arg\Gamma(l + 1 + iz/k)$ is the Coulomb phase shift. It therefore decreases exponentially along the curve $r = r_A \to r_A + i\infty$. Both $s_c(r)$ and $c_c(r)$ oscillate along this same line, and so the integrals

$$\int_{r_A}^{r_A + i\infty} dr e_o^+(r) \frac{\alpha}{r^2} s_c(r), \tag{A4a}$$

$$\int_{r_A}^{r_A + i\infty} dr e_o^+(r) \frac{\alpha}{r^2} c_c(r), \tag{A4b}$$

are well defined. By considering the infinite quarter circle joining this line with the line $r = r_A \to \infty$, and using the form of $e^+(r)$ in Eq. (24), we can equate the integrals Eqs. (A1a), (A1c) with the imaginary and real parts of the integral Eq. (A4a), and likewise we can equate the integrals Eqs. (A1b), (A1d) with the imaginary and real parts of the integral Eq. (A4b). In doing so, we have disregarded the divergent part of the integrals along the quarter circle

$$\oint e_o^+(r) \frac{\alpha}{r^2} s_c(r), \qquad \oint e_o^+(r) \frac{\alpha}{r^2} s_c(r), \tag{A5}$$

since, when we form the physical closed-channel solution [42],

$$e_c^-(r) = s_c(r) \cos \pi\nu - c_c(r) \sin \pi\nu, \tag{A6}$$

these divergences cancel, i.e., we are then left only with integrals of the form

$$\oint e_o^+(r) \frac{\alpha}{r^2} e_c^-(r), \tag{A7}$$

the integrand of which is zero everywhere on the quarter-circle contour at infinity. Finally, the integrals in Eqs. (A4) are evaluated numerically up to the point where the integrands have decayed beyond significance.

[1] N. R. Badnell *et al.* in *Atomic Processes in Plasmas*, edited by W. L. Rowan, AIP Confer. Proc. No. 322 (AIP, New York, 1995), p. 84.

[2] A. H. Gabriel and C. Jordan, in *Case Studies in Atomic Collision Physics II*, edited by M. R. C. McDowell and E. W. McDaniel (North-Holland, Amsterdam, 1972), p. 211.

[3] *Recombination of Atomic Ions*, Vol. 296 of *NATO Advanced Study Institute, Series B: Physics*, edited by W. G. Graham, W. Fritsch, Y. Hahn, and J. A. Tanis (Plenum, New York, 1992).

[4] L. H. Andersen, P. Hvelplund, H. Knudsen, and P. Kvistgaard, Phys. Rev. Lett. **62**, 2656 (1989).

[5] H. Danared, G. Andler, L. Bagge, C. J. Herrlander, J. Hilke, J. Jeansson, A. Källberg, A. Nilsson, A. Paál, K.-G. Rensfelt, U. Rosengård, J. Starker, and M. af Ugglas, Phys. Rev. Lett. **72**, 3775 (1994).

[6] J. Richard Mowat, H. Danared, G. Sundström, M. Carlson, L. H. Andersen, L. Vejby-Christensen, M. af Ugglas, and M. Larsson, Phys. Rev. Lett. **74**, 50 (1995).

[7] D. A. Knapp, R. E. Marrs, S. R. Elliott, E. W. Magee, and R. Zasadzinski, Nucl. Instrum. Methods Phys. Res. A **334**, 305 (1993).

[8] D. A. Knapp, P. Beiersdorfer, M. H. Chen, J. H. Scofield, and D. Schneider, Phys. Rev. Lett. **74**, 54 (1995).

[9] See, for example, Y. Hahn, Adv. At. Mol. Phys. **21**, 123 (1985).

[10] M. D. Hershkowitz and M. J. Seaton, J. Phys. B **6**, 1176 (1973).

[11] R. D. Cowan, J. Phys. B **13**, 1471 (1980).

[12] M. H. Chen, K. J. Reed, and D. L. Moores, Phys. Rev. Lett. **64**, 1350 (1990).

[13] N. R. Badnell, M. S. Pindzola, and D. C. Griffin, Phys. Rev. A **43**, 2250 (1991).
[14] J. Gau and Y. Hahn, J. Quant. Spectrosc. Radiat. Transfer **23**, 121 (1980).
[15] K. J. LaGattuta, Phys. Rev. A **40**, 80 (1989).
[16] S. L. Haan and V. L. Jacobs, Phys. Rev. A **40**, 80 (1989).
[17] M. S. Pindzola, F. Robicheaux, N. R. Badnell, M. H. Chen, and M. Zimmermann, Phys. Rev. A **52**, 42 (1995).
[18] D. C. Griffin, M. S. Pindzola, F. Robicheaux, T. W. Gorczyca, and N. R. Badnell, Phys. Rev. Lett. **27**, 3491 (1994).
[19] M. J. Seaton, Proc. R. Soc. London. Ser. A **218**, 400 (1953).
[20] P. C. W. Davies and M. J. Seaton, J. Phys. B **2**, 757 (1969).
[21] R. H. Bell and M. J. Seaton, J. Phys. B **18**, 1589 (1985).
[22] A. K. Pradhan and M. J. Seaton, J. Phys. B **18**, 1631 (1985).
[23] K. Sakimoto, M. Terao, and K. A. Berrington, Phys. Rev. A **42**, 291 (1990).
[24] S. N. Nahar and A. K. Pradhan, Phys. Rev. A **49**, 1816 (1994).
[25] F. Robicheaux, T. W. Gorczyca, M. S. Pindzola, and N. R. Badnell, Phys. Rev. A **52**, 1319 (1995).
[26] T. W. Gorczyca, F. Robicheaux, M. S. Pindzola, and N. R. Badnell, Phys. Rev. A **52**, 3852 (1995).
[27] T. W. Gorczyca and N. R. Badnell, J. Phys. B **29**, L283 (1996).
[28] N. R. Badnell, J. Phys. B **19**, 3827 (1986).
[29] D. C. Griffin, M. S. Pindzola, and C. Bottcher, Phys. Rev. A **33**, 3124 (1986).
[30] P. G. Burke and W. D. Robb, Adv. At. Mol. Phys. **11**, 143 (1975).
[31] P. G. Burke and K. A. Berrington, *Atomic and Molecular Processes: An R-matrix Approach* (IOP, Bristol, 1993).
[32] K. A. Berrington, P. G. Burke, K. Butler, M. J. Seaton, P. J. Storey, K. T. Taylor, and Yu Yan, J. Phys. B **20**, 6379 (1987).
[33] K. A. Berrington, W. B. Eissner, and P. H. Norrington, Comput. Phys. Commun. **92**, 290 (1995).
[34] N. S. Scott and P. G. Burke, J. Phys. B **13**, 4299 (1980).
[35] N. S. Scott and K. T. Taylor, Comput. Phys. Commun. **25**, 347 (1982).
[36] D. G. Hummer, K. A. Berrington, W. B. Eissner, A. K. Pradhan, H. E. Saraph, and J. A. Tully, Astron. Astrophys. **279**, 298 (1993).
[37] F. Robicheaux and C. H. Greene, Phys. Rev. A **48**, 4429 (1993).
[38] K. Bartschat and C. H. Greene, J. Phys. B **26**, L109 (1993).
[39] A. P. Hickman, J. Phys. B **17**, L101 (1984).
[40] N. C. Sil, M. A. Crees, and M. J. Seaton, J. Phys. B **17**, 1 (1984).
[41] M. J. Seaton, J. Phys. B **18**, 2111 (1985).
[42] M. J. Seaton, Rep. Prog. Phys. **46**, 167 (1983).
[43] S. Schennach, A. Müller, O. Uwira, J. Haselbauer, W. Spies, A. Frank, M. Wagner, R. Becker, M. Kleinod, E. Jennewein, N. Angert, P. H. Mokler, N. R. Badnell, and M. S. Pindzola, Z. Phys. D **30**, 291 (1994).
[44] P. H. Norrington and I. P. Grant, J. Phys. B **14**, L261 (1981).
[45] P. H. Norrington and I. P. Grant, J. Phys. B **20**, 4869 (1987).